Pergamon

Journal of Structural Geology, Vol. 16, No. 11, pp. 1575 to 1588, 1994

0191-8141/94 $07.00 + 0.00

0191-8141(94)00053-0

Strain modeling of displacement-field partitioning in transpressional orogens

BASIL TIKOFF and CHRISTIAN TEYSSIER

Department of Geology and Geophysics, University of Minnesota, Minneapolis, MN 55455, U.S.A.

(*Received* 31 *August* 1993; *accepted in revised form* 12 *April* 1994)

Abstract—In regions of oblique plate convergence, deformation is generally partitioned into strike-slip and contractional components. We use a strain model of transpression, based upon a three-dimensional velocity gradient tensor, to address the question of why such partitioning occurs. An exact relationship between angle of plate convergence, *instantaneous* strain, and *finite* strain is calculated, providing a predictive tool to interpret the type and orientation of geological structures in zones of oblique convergence. The instantaneous and finite strain axes are not coincident, and thus there is no simple relationship between instantaneous strain (or stress) and structures that developed over a protracted deformation, such as crustal-scale faults. In order to simulate more realistic geological settings, we use a partitioning model of transpression which quantifies the effect of fault efficiency on the displacement field. This model is applied to two transpressional settings: Sumatra and central California. Sumatra shows a very low degree of partitioning of the displacement field and a relatively small offset on the Great Sumatran fault. In contrast, central California displays a large degree of displacement partitioning, and efficient slip on the San Andreas fault system. Since both systems show partitioning of deformation into strike-slip and thrust motion, it is unlikely that the San Andreas fault is rheologically 'weaker' than the Great Sumatran fault. We propose that the difference in fault efficiency results from kinematic partitioning of the displacement field controlled by relative plate motion, rather than mechanical decoupling generated by fault weakness.

INTRODUCTION

As a better understanding of orogenic systems is developed, it is commonly recognized that partitioning of deformation occurs in a variety of plate tectonic settings. In many orogenic belts, both ancient—e.g. Cordillera (Oldow *et al.* 1989), Sierra Nevada (Tikoff & Teyssier 1993), Hercynides (Vauchez & Nicolas 1991)—and modern—e.g. San Andreas (Zoback *et al.* 1987, Mount & Suppe, 1987), Sumatra (Fitch 1972, Mount & Suppe 1992), Philippines (Pinet & Cobbold 1992), Eastern Turkey (Jackson 1992), New Zealand (Cashman *et al.* 1992, Walcott 1984)—deformation is partitioned into strike-slip and thrust-fault deformation. This phenomenon of partitioning has been approached in two distinct ways, either by assuming that stress is partitioned (e.g. Zoback *et al.* 1987, Rice 1992, Zoback & Healy 1992) or that strain is partitioned (e.g. Oldow 1990, Molnar 1992). The proponents of stress partitioning argue that weak faults embedded in a strong crust cause the maximum horizontal stress to be sub-perpendicular to the plate boundary. They maintain that the stress field in central California, for instance, is primarily controlled by fault properties and not plate motion. In this paper, we choose the alternative approach, and propose that plate motion primarily controls deformation in orogens. We use displacement-field partitioning of oblique plate convergence to investigate the geological and geophysical characteristics of transpressional plate boundaries.

We argue that deformation partitioning must ultimately be related to the relative motion of tectonic plates, although this relation is not necessarily simple. In this paper, exact relationships between relative plate motion, instantaneous strain orientations, and finite strain are calculated for transpressional zones, providing a predictive tool to interpret the type and orientation of geological structures developed in oblique convergence. Our investigation suggests that kinematic strain partitioning can explain most orogen-parallel and orogen-perpendicular structures of transpressional orogenic belts, such as those in central California and Sumatra.

This kinematic analysis also provides a quantitative tool to understanding the mechanics of oblique convergence: i.e. the fundamental difference between kinematic partitioning and mechanical decoupling. Partitioning is the kinematic response of a deformation system to applied boundary conditions. Decoupling implies mechanical independence of variables and the inability of a system to 'communicate' with far-field boundary conditions. If strain partitioning occurs, and deformation is primarily controlled by plate motion, a transpressional system may be either decoupled or coupled. For example, Mount & Suppe (1987, 1992) suggest that relative plate motion controls the deformation in central California, but adjacent sides of the San Andreas fault are 'decoupled' due to the presence of a 'weak' San Andreas fault. Alternatively, Molnar (1992) proposed that shearing of the upper mantle over a wide area below the San Andreas system effectively 'couples' the adjacent sides of the fault. Our kinematic analysis applied to

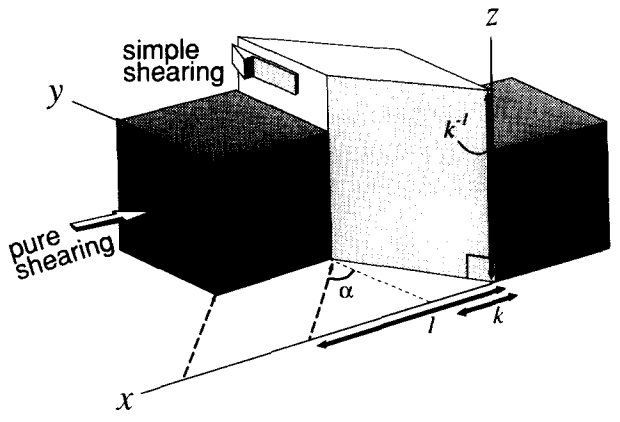

Fig. 1. Transpression model. Two rigid blocks (dark gray) converge obliquely in a reference system, defining a transpressional zone of deformation (light gray). k and k^{-1} represent the pure shear component of deformation and α denotes the angle of convergence.

Sumatra and central California suggests that transpressional systems partition deformation within a coupled system, without the necessary existence of weak faults.

STRAIN MODELING

A detailed understanding of transpressional–transtensional systems requires precise strain models that address both instantaneous and finite strain. Sanderson & Marchini (1984) provided a finite strain solution which predicts the orientations of lines and planes for a given finite strain ellipsoid. Little attention has been paid to instantaneous strain quantities which might be applicable, for instance, to present-day structures at plate boundaries. In order to fully describe the three-dimensional, non-plane strain, and non-coaxial nature of transpression and transtension, it is necessary to define both a deformation and velocity gradient tensors, as well as their relationship to instantaneous and finite strain. Tikoff & Fossen (1993) followed the method of Ramberg (1975), and developed a general three-dimensional deformation matrix. Fossen & Tikoff (1993) applied this matrix to the relatively simple case of transpressional and transtensional tectonics, using simultaneously a vertical simple shear (wrench in the x-direction) combined with a pure shear in the y–z plane (Fig. 1). The constraints of the Sanderson & Marchini (1984) transpressional model—homogeneous deformation, free upper surface, fixed lower surface, and no volume change—were also adopted in the modeling. Using a velocity gradient tensor for transpression given by

$$\mathbf{L} = \begin{pmatrix} 0 & \dot{\gamma} & 0 \\ 0 & \dot{\varepsilon} & 0 \\ 0 & 0 & -\dot{\varepsilon} \end{pmatrix} \quad (1)$$

where $\dot{\varepsilon}$ and $\dot{\gamma}$ are the strain rates for pure and simple shear, respectively (see Appendix 1 for a list of variables), it was shown that the deformation tensor, for an exact combination of pure and simple shearing, is given by

$$\mathbf{D} = \begin{pmatrix} 1 & \dfrac{\gamma(1-k)}{\ln(k^{-1})} & 0 \\ 0 & k & 0 \\ 0 & 0 & k^{-1} \end{pmatrix} \quad (2)$$

where k is the amount of pure shear component that acts in the horizontal (x) direction which is compensated by the elongation k^{-1} in the vertical (z) direction. The shear strain γ describes the simple shear component of deformation. The finite strain ellipsoid associated with equation (2) can be found by taking the eigenvalues and eigenvectors of the matrix $\mathbf{DD}^{\mathrm{T}}$. The eigenvalues give the magnitude of the maximum (λ_1), intermediate (λ_2), and minimum (λ_3) axes of the finite strain ellipsoid, while the eigenvectors give their orientation (Flinn 1979, Tikoff & Fossen 1993).

The advantage of the decomposition of the deformation matrix used by Tikoff & Fossen (1993) is that instantaneous and finite strains can be correlated. The finite strain terms, k and γ, relate to instantaneous quantities as follows:

$$k = \exp(\dot{\varepsilon}t) \quad \text{or } \dot{\varepsilon} = \frac{\ln(k)}{t} \quad (3a)$$

and

$$\dot{\gamma} = \frac{\gamma}{t}. \quad (3b)$$

In particular, we would like to know how to correlate the finite strain ellipsoid with the instantaneous strain axes: $\dot{s}_1 > \dot{s}_2 > \dot{s}_3$ or instantaneous stretching axes (ISA; e.g. Passchier 1988). We can calculate the instantaneous strain by substituting infinitesimal values into the deformation matrix $\mathbf{D}$. The same result is obtained by taking the eigenvectors and eigenvalues of the stretching tensor $\dot{\mathbf{S}}$, which are the orientation and magnitude, respectively, of the instantaneous strain axes (Malvern 1969, Tikoff & Fossen 1993).

On the basis of the orientation of the instantaneous stretching axes, Fossen & Tikoff (1993) defined two types of transpression and two types of transtension (Fig. 2): wrench-dominated and pure-shear dominated. In this paper, we focus on transpression. In pure-shear dominated transpression, $\dot{s}_2$ and $\dot{s}_3$ lie in the horizontal plane and are oblique to the shear (x–z) plane, and $\dot{s}_1$ is vertical. Notice that the instantaneous strain ellipsoid is constant during a steady-state deformation. The finite strain ellipsoid starts parallel to the instantaneous strain, but λ_2 and λ_3 progressively rotate to become parallel and perpendicular, respectively, to the shear plane at infinite strain. This rotation is due to the non-coaxial nature of the simple shear component.

In wrench-dominated transpression, $\dot{s}_1$ and $\dot{s}_3$ lie in the horizontal plane and oblique to the shear plane, while $\dot{s}_2$ is vertical. During steady-state deformation, the finite strain axes start parallel to the instantaneous strain axes, so λ_1 and λ_3 lie in the horizontal plane, and λ_2 is vertical. However, after some deformation, λ_1 switches with λ_2 and becomes vertical. The amount of deformation it

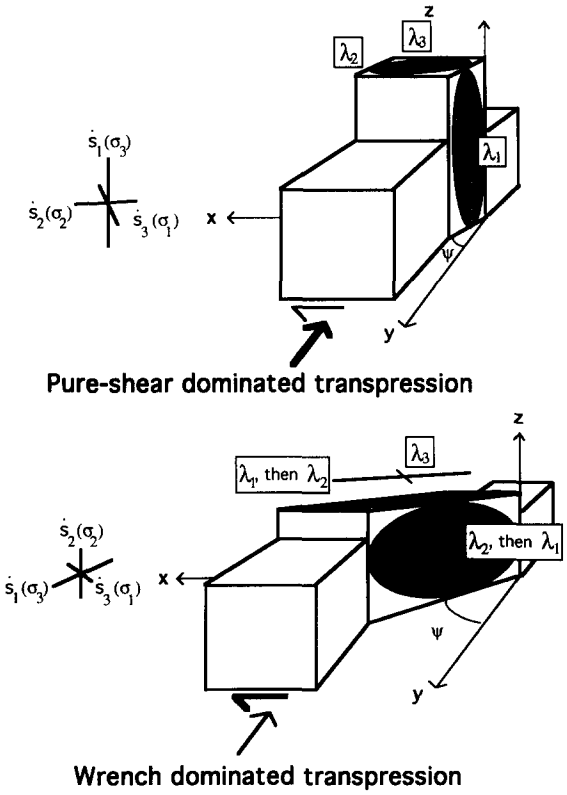

Fig. 2. Two types of transpression, distinguished by the orientation of instantaneous strain axes. In pure-shear dominated transpression, the pure-shear component dominates both the instantaneous and finite strain. Wrench-dominated transpression results in a misorientation of finite and instantaneous strain axes after some deformation, because the instantaneous pure-shear component, although smaller than the simple-shear component, is more efficient at accumulating finite strain (see Fig. 3). Note that instantaneous strains are often correlated with stresses.

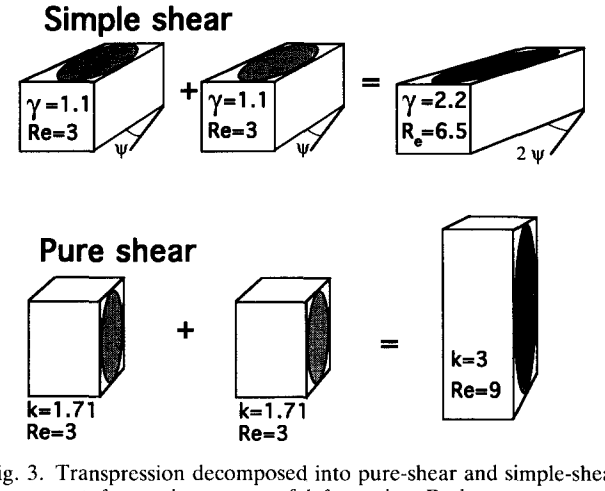

Fig. 3. Transpression decomposed into pure-shear and simple-shear components for two increments of deformation. Both components are incrementally equal, but the coaxial nature of pure shear causes larger finite deformation (R_e is the ratio of the long over short axes of the strain ellipsoid), resulting in finite and instantaneous strains axes lying at 90° from one another in wrench-dominated transpression.

takes to arrive at this switch is dependent on the relative magnitudes of the pure-shear and simple-shear components of transpression (Fig. 3). The pure-shear component that elongates material in the vertical direction adds multiplicatively. The simple-shear component, although it is incrementally larger, adds less effectively

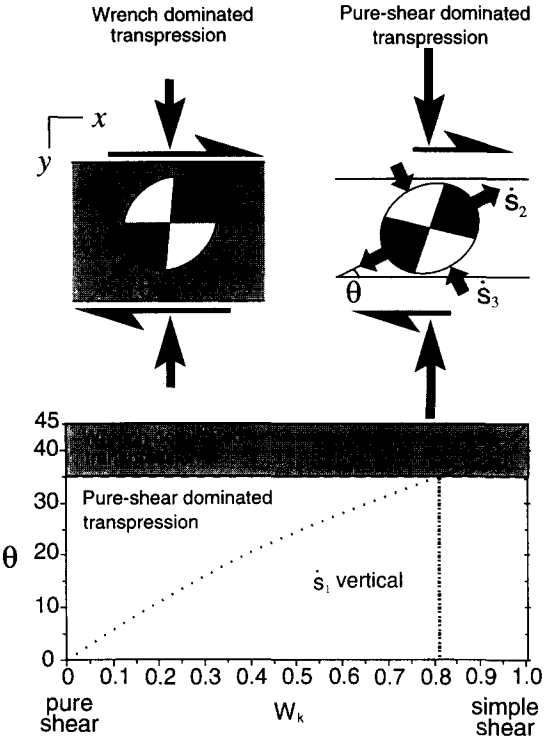

Fig. 4. Relationship between kinematic vorticity number, W_k, and the angle θ between the maximum horizontal axis of the instantaneous strain ellipsoid and the deformation zone boundary (Fossen & Tikoff 1993). Wrench-dominated and pure-shear dominated transpression are defined on the basis of the orientation of the instantaneous strain axes. The transition occurs at $W_k = 0.81$ and $\theta = 35°$.

than the pure-shear component because the finite strain axes are not parallel to the instantaneous strain axes. The larger the component of simple-shear deformation, the more strain must accumulate before the maximum and intermediate axes of the finite-strain ellipsoid switch positions. However, it is important to realize that, after this switch occurs, not only are the principal axes of the instantaneous and finite strain ellipsoids not parallel due to the non-coaxial nature of flow (i.e. $\dot{s}_3$ is not parallel to λ_3), but the principal planes are no longer coincident (i.e. the plane containing λ_1 and λ_3 is vertical, the plane containing $\dot{s}_1$ and $\dot{s}_3$ is horizontal).

In order to distinguish quantitatively between wrench and pure-shear dominated transpression, we use the kinematic vorticity number (W_k; Truesdell 1953). This number simply records a non-linear ratio of the pure to simple shear components during deformation. For a transpressional deformation, W_k is given by,

$$W_k = \frac{\dot{\gamma}}{\sqrt{4\dot{\varepsilon}^2 + \dot{\gamma}^2}} \tag{4a}$$

or, in terms of finite strain values,

$$W_k = \frac{\gamma}{\sqrt{4\ln(k)^2 + \gamma^2}} \tag{4b}$$

(Tikoff and Fossen 1993). The angle θ between the minimum instantaneous strain axis $\dot{s}_3$ and the transpressional zone boundary corresponds to a unique W_k (Fig. 4). We use the orientation of $\dot{s}_3$ since it remains horizontal during both wrench- and pure-shear dominated

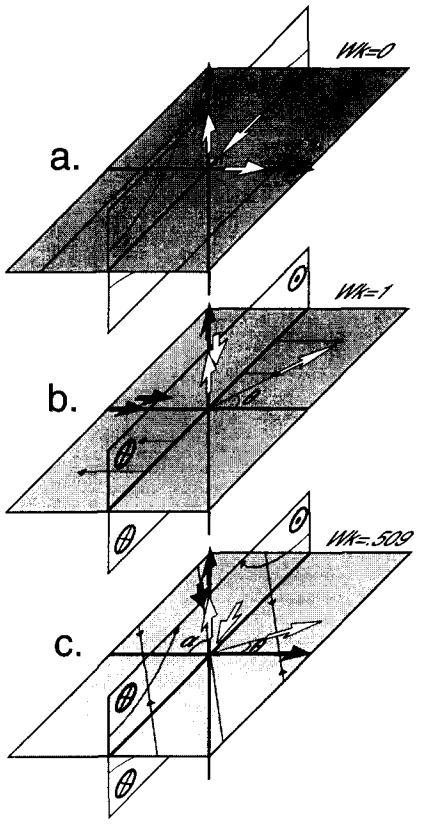

Fig. 5. Relationship between flow apophyses (black arrows), instantaneous strain axes (white arrows), and flow lines (thin lines with arrows), for (a) pure shear ($W_k = 0$), (b) simple shear ($W_k = 1$), and (c) a particular transpressional case ($W_k = 0.509$). α is the angle between the contractional flow apophysis and the x-axis.

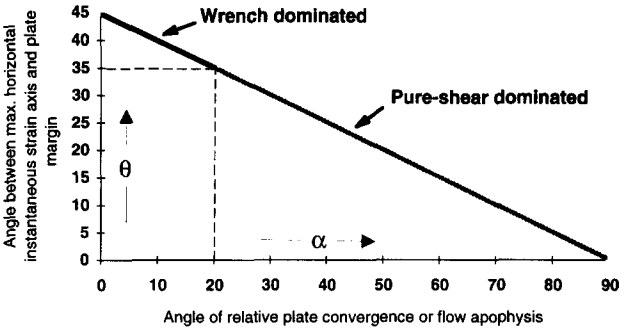

Fig. 6. Relationship between the angle α of plate convergence (direction of the contractional flow apophysis) and the angle, θ, that the maximum horizontal axis of incremental strain ellipsoid makes with the plate margin (see Fig. 4). The transition between wrench-dominated and pure-shear dominated transpression occurs at an angle of convergence of 20°.

transpression. It can be shown that $\dot{s}_1$ is vertical for $0.81 < W_k \leq 1$ and horizontal for $0 < W_k \leq 0.81$. Therefore, wrench-dominated transpression is defined when $1 > W_k > 0.81$ and $35° < \theta < 45°$ while for pure-shear dominated transpression, $0.81 \geq W_k > 0$ and $0° < \theta < 35°$ (Fossen & Tikoff 1993).

RELATIONSHIP BETWEEN PLATE MOTION AND STRAIN IN TRANSPRESSIONAL ZONES

The relationship between plate motion and strain can be quantified by assuming that plate boundaries are transpressional systems in zones of oblique convergence, pure transform movement and normal convergence being end-members. This simple, but physically and geologically reasonable assumption allows us to define the direction of relative plate motion as a flow apophysis of a homogeneous continuum (McKenzie & Jackson 1983). Flow apophyses are the eigenvalues of the velocity gradient tensor (Bobyarchick 1986), i.e. the directions of greatest gradient of velocity. There are two flow apophyses for plane-strain deformation and three flow apophyses for non-plane strain deformation. In transpression, one flow apophysis is always contractional and horizontal, one is neutral and parallel to the x-axis in the horizontal plane, and one is extensional and parallel to the vertical z-axis (Fig. 5). Assuming that the direction of plate motion controls the displacement field in the transpressional zone, the relative motion vector must be parallel to the contractional flow apophysis. Note that the flow apophyses, unlike strain ellipsoid axes, need not be mutually perpendicular.

What is the relationship between the orientation of the contractional flow apophysis and the minimum axis of the instantaneous strain ellipsoid ($\dot{s}_3$)? Examples of plane strain cases illustrate that flow apophyses and strain axes are generally non-coincident, except in pure shear (Fig. 5a), where $\dot{s}_3$ is parallel to the contractional flow apophysis. In simple shear (Fig. 5b), $\dot{s}_3$ is oriented at 45° to the shear direction, while both horizontal flow apophyses are parallel to the shear direction. Weijermars (1991) has shown for plane strain cases of combined pure and simple shear, that a linear relation exists between the orientation of the flow apophyses and the axes of the instantaneous strain ellipsoid. Only in the case of pure shear do movement direction and instantaneous strain direction coincide.

Displacement within a homogeneous transpressional zone is defined by the quantities of the velocity gradient tensor $\mathbf{L}$ (McKenzie & Jackson 1983). It follows from equation (1) that the three flow apophyses for transpressional deformation are:

$$\begin{pmatrix}1\\0\\0\end{pmatrix}, \quad \begin{pmatrix}\frac{-\gamma}{\dot{\varepsilon}}\\1\\0\end{pmatrix}, \quad \begin{pmatrix}0\\0\\1\end{pmatrix}. \tag{5}$$

Using this relationship, and substituting small values of pure- and simple-shear components of deformation into the deformation matrix (equation 2), a linear relationship between flow apophyses and orientation of the minimum axis of instantaneous strain is derived (Fig. 6), as was also shown by Jamison (1991). This linear relationship is similar to the plane strain case, which is not surprising since the instantaneous strain is a direct result of the relative displacement of material points in the planes that contain the flow apophyses. However, for a given orientation of the flow apophysis, the W_k value is always lower in transpressional cases compared to plane strain, due to the movement of material out of the horizontal plane. The relationship between W_k, flow

apophyses, and direction of instantaneous strain axes is shown diagramatically for particular cases of transpression in Fig. 5(c). The relationship between flow apophyses and instantaneous strain axes is continuous through the transition between wrench dominated and pure-shear dominated transpression, as this transition is solely a function of the relative magnitudes of $\dot{s}_1$ and $\dot{s}_2$, and does not affect $\dot{s}_3$.

INSTANTANEOUS STRAIN AND RELATIVE PLATE MOTION

Applying the above analysis to transpressional plate boundaries, and assuming homogeneous deformation, it is possible to predict the exact relationship between the orientation of the instantaneous stretching axes and the direction of relative plate motion. In pure convergence the relative plate-motion direction and the minimum axis of instantaneous strain coincide ($\alpha=90°$, $\theta=0°$). In pure wrench deformation, $\alpha=0°$, and $\theta=45°$. Between these two end-members, an entire range of possibilities exists (Fig. 6). Therefore, a 'refraction' of the instantaneous strain axes occurs with respect to the direction of relative plate motion.

Several physical experiments of oblique tectonics have reproduced this refraction between direction of relative motion and strain axes as traced, for example, by the trend of initial faults (Withjack & Jamison 1986, Richard & Cobbold 1990, Tron & Brun 1991). Unfortunately for the purpose of this discussion, most of these experiments simulated oblique rifting (or transtension). Transtension, however, is the exact numerical inverse of transpression (Fossen & Tikoff 1993), with the same subdivisions of pure-shear and wrench-dominated transtensional deformation, such that a refraction of instantaneous axes is also expected. The refraction of strain axes produced during the experiments of Withjack & Jamison (1986) closely matches our analytical predictions.

FINITE VS INSTANTANEOUS STRAIN, AND PARTITIONING OF GEOLOGICAL STRUCTURES

Because the instantaneous and finite strain ellipsoids can be substantially non-parallel during transpressional deformation, it is important to discuss whether geologic structures reflect instantaneous or finite strain. For simplicity, we first discuss a case of homogeneous, wrench-dominated transpression, such as may occur in a vertical ductile shear zone. In this case, the instantaneous strain is close to that expected for strike-slip, and the maximum instantaneous stretching direction ($\dot{s}_1$) is horizontal. However, within the same zone of steady-state deformation, the finite strain ellipsoid, after showing pure flattening, records a vertical λ_1. Therefore, the finite strain markers—such as boudinaged clasts/veins, elongated fossils, stretching lineations—probably show vertical extension while the instantaneous strain (stress) axes are consistent with dominantly strike-slip motion (Simpson & De Paor 1993, Fossen & Tikoff 1993).

Consider the case where bulk homogeneous transpressional deformation must be accommodated by faulting, as seen in the brittle realm of active orogens. As a first approximation, we assume that initial faulting in a homogeneous block is controlled by the orientation of the instantaneous strain responding to the initial movement of material points. Once formed, these structures are likely to be preferentially reactivated. If the orientation of primary faults is controlled by the orientation of the instantaneous stretching axes, these faults should form in different orientations for pure-shear and wrench-dominated transpression. In pure-shear dominated transpression, $\dot{s}_1$ and $\dot{s}_3$ lie in a vertical plane and reverse faults should form. Since $\dot{s}_1$ and $\dot{s}_3$ lie in the horizontal plane during wrench dominated transpression, strike-slip faults are expected to develop first. This result was again corroborated by physical experiments. Withjack & Jamison (1986) reported primary formation of strike-slip faults for $\alpha=0°$ and 15° (wrench-dominated transtension), and primary formation of normal faults for $\alpha=30°$, 45°, 60°, 75° and 90° (pure-shear dominated transtension). While the relative magnitudes of the instantaneous strain axes may play some role in the attitude of initial faults, not enough is known about three-dimensional, non-coaxial strain to take this effect into account.

Therefore, boundary conditions appear to control the types and orientations of faults that initially form during deformation. However, if bulk finite strain must also be accommodated by faulting and fracturing, complex relations might develop. Consider the case of a material undergoing wrench-dominated transpression. The instantaneous strain axes, throughout the entire deformation, are oriented consistent with strike-slip movement. However, due to the non-plane strain aspect of transpressional deformation, finite strain records an increased component of pure shear. If deformation continues to large strain values, even with a small pure-shear component, the geometry of the finite strain ellipsoid is consistent with predominantly contractional motion: λ_1 and λ_2 lie in the horizontal plane, and λ_3 is vertical.

If faults form only as a result of instantaneous strain, all faults in wrench-dominated transpression must be vertical to accommodate strike-slip displacement. However, vertical faults cannot accommodate the contraction across the deforming zone imposed by finite strain. Therefore, thrust faults striking near-parallel to the orogen must form to accommodate finite rather than instantaneous strain. Once strike-slip and thrust faults are formed, they will continue to be active during deformation because they are well oriented to accommodate the transcurrent and contractional components of deformation, respectively. Therefore, we expect strike-slip and reverse faults to be active simultaneously during orogenic processes.

A similar situation occurs for pure-shear dominated transpression. In this setting, thrust faults form first, in

response to the applied instantaneous strain. However, once formed, the thrust faults are not well oriented to accommodate the strike-slip movement imposed by the transpressional boundary conditions. Therefore, strike-slip faults form in response to finite strain, rather than instantaneous strain. As deformation continues, both thrust and strike-slip faults should be active to accommodate the imposed displacement gradient which contains components of contractional and transcurrent movement.

These analytical results, supported by physical experiments, form the basis of the idea of strain partitioning. Material must respond to accommodate finite strain, which may be substantially misoriented relative to the instantaneous strain field. While such a misorientation obviously occurs in geometrical obstacles, such as lateral ramps in a thrust fault system, it can also occur in homogeneous, transpressional deformation because of the boundary conditions of deformation. This result is a logical extension of the two-dimensional analysis of Wojtal (1989) who suggested that structures, even in the brittle regime, are consistent with the imposed displacement gradient.

This analysis also emphasizes the overlooked importance of boundary conditions in geological analyses. While many studies implicitly or explicitly rely on stress orientation (e.g. Anderson 1951, Rice 1992), stress may, in general, be less important than the kinematic boundary conditions that control deformation, even in the brittle realm. If we accept that finite strain imposed by the boundary conditions, rather than stresses, control fault movement, then there is no simple relationship between instantaneous strain and large-scale faulting. Large-scale faults are better described in the context of the three-dimensional velocity gradient tensor and are controlled by the relative movement of material points rather than the applied stresses.

OBSERVATIONS FROM PHYSICAL EXPERIMENTS

Physical experiments corroborate this type of partitioning. For instance, sand experiments of oblique convergence conducted by Pinet & Cobbold (1992), where the boundary conditions of deformation were kept constant, correlate with pure-shear dominated transpression (α generally greater than 20°). These experiments show that thrust faults form early (interpreted as a response to the instantaneous strains) and strike-slip faults develop later (inferred as a result of finite strain).

In a series of important experiments, Richard & Cobbold (1989, 1990) created flower structures and partitioning of deformation into strike-slip and thrust faulting when a layer of sand was placed upon a layer of silicon, which acted as a Newtonian fluid. When a layer of sand was placed on a sheet of mylar, oblique slip was more common. Richard & Cobbold (1989, 1990) explained this partitioning by suggesting that the sand, which acted as a Coulomb material, was weak toward the upper free surface and that there were nearly horizontal tractions imposed by the viscous silicon substrate. Molnar (1992) interprets these experiments differently. He suggests that the viscous silicon layer acted to 'smooth' the relative displacement into a wide, continuous zone of transpression, and effectively coupled the sand and the basal velocity discontinuity. The fact that the strike-slip fault developed directly above the basal discontinuity located below the silicon substrate supports Molnar's interpretation.

These experimental results have several implications. First, both thrust faults and strike-slip faults can occur simultaneously in a single setting with well defined boundary conditions and constant imposed strain. Further, both the thrust and strike-slip faults must have the same strength, as they occur in the same material, and it is not necessary that the strike-slip fault be weak for thrust faults, striking parallel to the strike-slip fault, to form. Lastly, the results suggest that partitioning in transpression is particularly expected in crustal domains that are underlain by a basal shear or décollement. The results of these experiments cast serious doubt on the likelihood of stress partitioning occurring in transpressional settings.

STRAIN MODELING OF DEFORMATION PARTITIONING

Contractional and transcurrent structures are simultaneously active not only in physical experiments but also in most zones of oblique convergence (e.g. Fitch 1972). Because of this partitioning of deformation, a homogeneous strain approach is insufficient to quantify deformation of a complete transpressional system. Models of homogeneous strain are adequate to calculate the relative component of contraction vs transcurrent motion in areas that do not show much discrete faulting. Jamison (1991) uses a homogeneous strain analysis for a variety of wrench 'borderlands' which do not include major faults. In order to treat a whole system, we need an analytical tool that is capable of calculating homogeneous transpression and discrete, transcurrent offset.

If we assume that the displacement field within a transpressional plate margin is controlled by oblique plate motion, partitioning can be quantified as a function of the relative effects of distributed transpressional deformation and discrete slip (Fig. 7). We are restricting ourselves in this paper to the case of a transpression zone in which deformation is accommodated by discrete slip on orogen-parallel faults and distributed deformation in the segments between the faults. This situation is commonly encountered in oblique convergence, and allows us to compare our kinematic results with the mechanical models of weak faults proposed by Zoback *et al.* (1987).

The effect of the pure-shear component must be recorded in internal deformation, crustal thickening, and topographic relief, which explains the relative predominance of this component in the classical analyses of mountain building. The transcurrent component can be

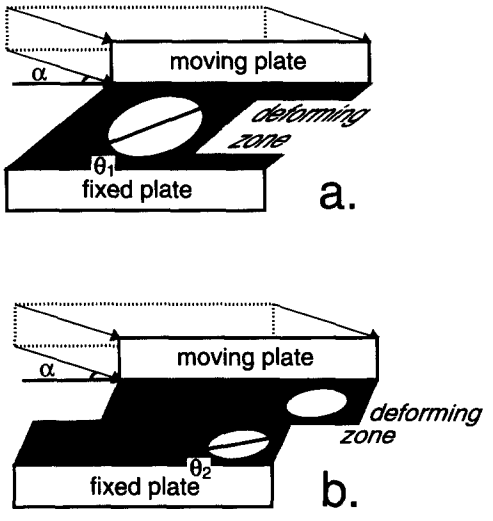

Fig. 7. Schematic diagram of two plates converging at an angle α, and the resulting transpressional plate boundary characterized by (a) distributed, and (b) partitioned displacement. If partitioning occurs, the angle θ_2 is always smaller than θ_1; i.e. the deformed zone contains a larger component of pure shear compared to the non-partitioned case.

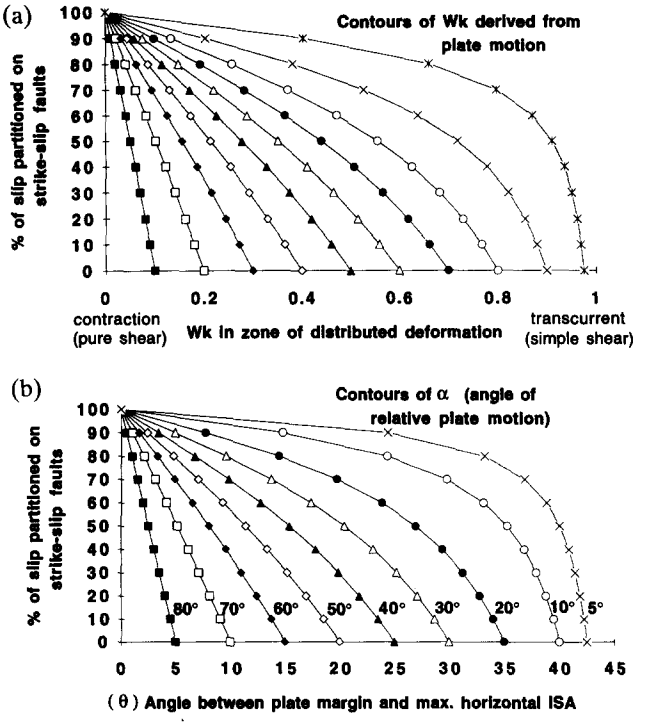

Fig. 8. (a) Relationship between bulk W_k imposed by plate motion and W_k within the zone of distributed deformation, as a function of the percentage of shear displacement taken up by discrete faults. (b) Relationship between the orientation of the maximum horizontal ISA (instantaneous strain axis) (θ in Figs. 4 and 7) and the angle of relative plate motion (shown for 5°–80°), as a function of displacement partitioning on discrete faults.

partitioned into both internal deformation and slip on discrete faults (Appendix 2) resulting in orogen-parallel transport. For any component of transcurrent motion that is partitioned into discrete strike-slip faults, the kinematic vorticity within the transpressional zone must decrease (i.e. become more contractional). Since discrete strike-slip takes up a part of the simple-shear component of the homogeneous transpression model, the relative role of the pure-shear component is increased (W_k decreases) in the homogeneously deformed segments.

Therefore, a relationship exists between bulk W_k predicted by plate motion, W_k recorded in the internally deformed transpressional zone, and the percentage of the simple-shear component accommodated by discrete slip on strike-slip faults (Fig. 8a). For plate motion dominated by normal to moderately oblique convergence, W_k of the transpressional zone decreases quite linearly with an increasing partitioning of the strike-slip component. For plate motion dominated by wrenching, W_k in the transpressional zone decreases more rapidly in a nonlinear manner, as a greater fraction of the simple-shear component is taken up by discrete strike slip. This result is associated with the more effective contribution of the pure-shear component of transpression to the overall W_k as more discrete strike-slip faulting accommodates the simple-shear component.

An equally correct and perhaps more applicable relationship also exists between the angle of relative plate convergence, the orientation of the instantaneous strain axes, and the percentage of discrete slip accommodated on strike-slip faults (Fig. 8b). The instantaneous strain, rather than the finite, is considered because it is independent of the amount of displacement. The maximum horizontal axis of instantaneous strain rapidly becomes near parallel to the transpressional zone boundary if partitioning is large, even in the case of wrench dominated transpression. Using this graph, it is possible to compute partitioning in the system if relative plate motion is known, and if the angle between geologically instantaneous structures can be measured. Conversely, if both plate motion and rate of slip on discrete faults are known, the orientation of instantaneous structures within the transpressional zone can be predicted, providing an independent test of the model.

APPLICATION TO TRANSPRESSIONAL PLATE BOUNDARIES

Sumatra and the Great Sumatran fault

Sumatra is a clear example of oblique convergence, defined by the relative motion between the Australian plate and the Eurasian plate (DeMets *et al.* 1990). A part of the oblique motion is taken up by the Great Sumatran fault which faithfully follows the attitude of the subduction plate boundary. The average convergence rate of 70–75 mm y^{-1} in Java where subduction is subperpendicular to the trench, can be decomposed into normal and lateral components along the Sunda arc to the northwest. The normal component decreases from 70–75 mm y^{-1} to 7–20 mm y^{-1} from Sunda Strait to the Andaman Sea, and the right-lateral component increases accordingly from 0 to 44–47 mm y^{-1} (Moore *et al.* 1980, after Minster & Jordan 1978). Given these boundary conditions, a gradual change from pure-shear dominated to wrench-dominated transpression is

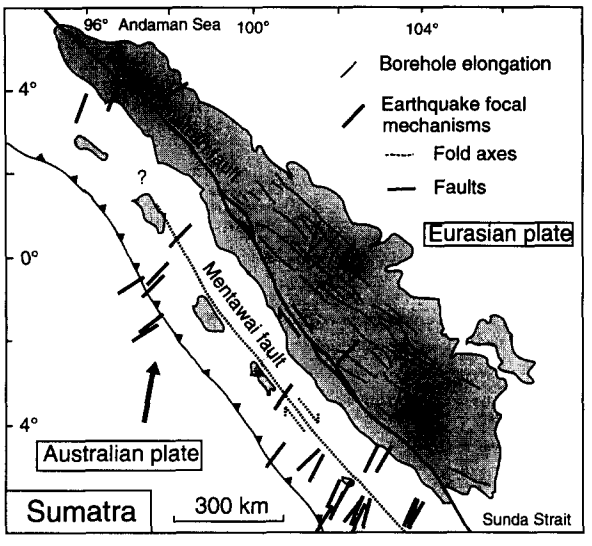

Fig. 9. Distributed deformation within Sumatra, associated with approximately 50° oblique convergence of Australian and Eurasian plates, based on Mount & Suppe (1992). Obliquity changes along strike, from Sunda strait to the Andaman Sea. The Great Sumatran and Mentawai faults demonstrate dextral motion. Orientations of borehole elongations (short lines), earthquake slip vectors (bold long lines), and fold axes in young sediments (dashed line), showing a consistent 15° (or 75°) obliquity to the Great Sumatran fault.

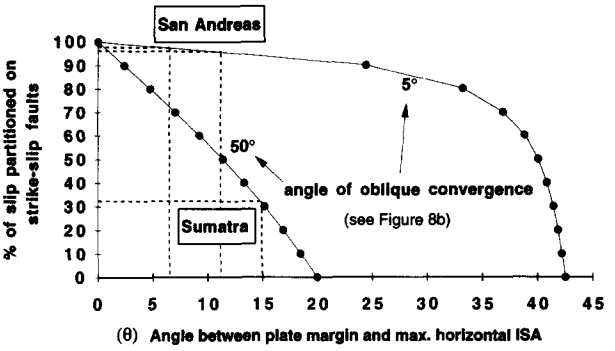

Fig. 10. Plot of the Sumatra and San Andreas cases in a strain partitioning graph. In Sumatra, the 15° angle between the structures that track the maximum horizontal instantaneous strain axis (ISA) and the plate boundary and the 50° convergence angle imply that about 33% of the strike-slip deformation is taken up by discrete faulting. In the case of the central region of the San Andreas system, the 6–12° structural obliquity (Fig. 11), and the 5° angle of plate convergence would predict that over 95% of the simple shear component should be taken up by discrete strike-slip faults.

expected to control deformation from south to north. McCaffrey (1991) proposed that a component of arc parallel stretching, increasing to the north, is accommodated in the fore arc, which might also reflect a greater contribution of dextral simple shear to the north.

The degree of displacement partitioning on discrete dextral faults is unclear. It is well established that total offset and slip rate on the Great Sumatran fault increase drastically from southeast Sumatra (50–70 km, 6 mm y^{-1}) (Lassal *et al.* 1989, Bellier *et al.* 1991) to the Andaman Sea (450 km, 40 mm y^{-1}) (Curray *et al.* 1979), where the fault breaks down into a series of transforms that accommodate the opening of oceanic spreading centers. However, it has also been proposed that other faults, such as the Mentawai fault off Sumatra, might also accommodate strike slip (Diament *et al.* 1992), but no slip rate is available.

Within the fore-arc region of Sumatra, seismic sections show SE-directed thrust faults (Karig *et al.* 1980) and associated folds (Diament *et al.* 1992), trending at relatively low angles to the plate margin, corroborated by slip vectors from earthquake focal mechanisms (McCaffrey 1991). In the back-arc region of the south and central regions of Sumatra, slip vectors, young folds, and borehole breakout data suggest a similar relationship (Fig. 9) (Mount & Suppe 1992). Therefore, within a deformation zone several hundred kilometers wide encompassing both sides of the Great Sumatran fault, an angle of approximately 15° is observed between geologic structures—young folds hinges, poles to dikes, and recent faults—and the Great Sumatran fault.

Assuming that Sumatra responds to bulk transpressional deformation, we apply the simple strain modeling of partitioning derived above. The angle between the relative plate motion vector and the subduction trench is approximately 50° (Minster & Jordan 1978), although it clearly changes along strike. Using the angle of plate convergence as a flow apophysis of the displacement field within the transpressional deforming zone, one would predict the direction of the maximum horizontal axes of the instantaneous strain ellipsoid to be about 20° from the orientation of the deforming transpressional shear zone boundary, taken as the Great Sumatran fault. If the axes of young folds, directions of borehole breakout, and seismic slip vector projections compiled by Mount & Suppe (1992) are taken to reflect instantaneous strain, it follows that the 15° obliquity of these structures with respect to the plate boundary indicates that approximately one-third of the strike-slip component of displacement is taken up by discrete strike-slip faulting (Fig. 10).

A test of the model would be the accurate knowledge of slip rates on the Great Sumatran fault in south and central Sumatra. The figure of 6 mm y^{-1} in South Sumatra (Bellier *et al.* 1991) might increase significantly in central Sumatra (McCaffrey 1991), but it is unlikely to come close to the 40 mm y^{-1} observed in the Andaman Sea. If a figure of 10–15 mm y^{-1} is adopted as a tentative average slip rate on the southern and central portions of the Great Sumatran fault, another 20–30 mm y^{-1} (the remaining two-thirds) of lateral motion should be accommodated by the simple-shear component distributed across the 300 km wide deformation zone. The total rate of dextral shear is comparable to the 45 mm y^{-1} lateral plate motion resolved on the oblique (50°) plate boundary converging at 70 mm y^{-1}. On the other hand, the absolute quantity of lateral displacement is dependent on the coupling between the descending slab and the transpressional wedge, making any further analysis highly speculative. The resolution of this problem will have to be a detailed analysis of the displacement field in the wedge using both geological and geophysical techniques to measure the components of accumulated normal shortening and translation, and geodetic surveys of the present-day displacement field.

It remains that a model of pure-shear dominated transpression for south and central Sumatra is consistent with the predominance of thrust faults in the wedge and the relatively sluggish motion on the Great Sumatran fault in that region. A drastic increase in slip rate from 6 to 40 mm y^{-1} on the fault toward the Andaman Sea is entirely consistent with the model, since the northern part of the system is controlled by wrench dominated transpression, similar to California.

California and the San Andreas fault system

Central California switched from a transcurrent to a transpressional plate boundary about 2.48 Ma, during a slight reorientation of relative plate motion (Harbert 1991). The San Andreas fault system actually consists of several faults, although most of the strike-slip motion is concentrated on the San Andreas fault which defines the plate boundary (Powell & Weldon 1992). A subhorizontal décollement is suspected to be present beneath the San Andreas fault system, evidenced by block rotation (Weldon & Humphreys 1986, McKenzie & Jackson 1983), seismic sections (Namson & Davis 1988, Bloch *et al.* 1993), and a 200 km wide high heat flow anomaly in central California (Lachenbruch & Sass 1973, 1980) suggesting shearing in the upper mantle (Molnar 1992). One notable difference with Sumatra is that deformation occurs within adjacent plates of continental crust and thus a higher degree of mechanical coupling on the scale of the lithosphere is likely. Therefore, a model of bulk transpression appropriately describes the San Andreas system.

The angle of oblique convergence between the North American and Pacific plates is approximately 5° at the latitude of central California (DeMets *et al.* 1990). Using a homogeneous strain modeling of transpression, the predicted angle between the long axis of instantaneous strain and the trace of the San Andreas fault should be 42.5° (Figs. 6 and 10), as in a wrench-dominated transpression system. However, structures such as upright young fold hinges and borehole breakouts are oriented nearly parallel to the fault. The lowest angle is recorded in central California, where breakout directions and fold axes lie at approximately 6° and 12°, respectively, to the San Andreas fault (Fig. 11) (Mount & Suppe 1987). Based upon these angles, strain modeling (Fig. 10) predicts that at least 95% of the wrench component of transpression should be taken up by discrete faults.

The existence of geodetic arrays along the San Andreas fault system allows a first approximation of slip accommodated by the fault, and therefore of displacement partitioning. Although studies vary, in general only about 70–75% of the 47.8 mm y^{-1} right lateral component (DeMets *et al.* 1990) induced by plate motion is accounted for by discrete strike slip on the San Andreas fault: 35 mm y^{-1} in the northern Bay area (Prescott & Yu 1986); 34 mm y^{-1} in the central, creeping section (Rymer *et al.* 1984); and 30 mm y^{-1} in the big bend area (Eberhart-Phillips *et al.* 1990). However, significant slip occurs on other discrete faults: the Hosgri

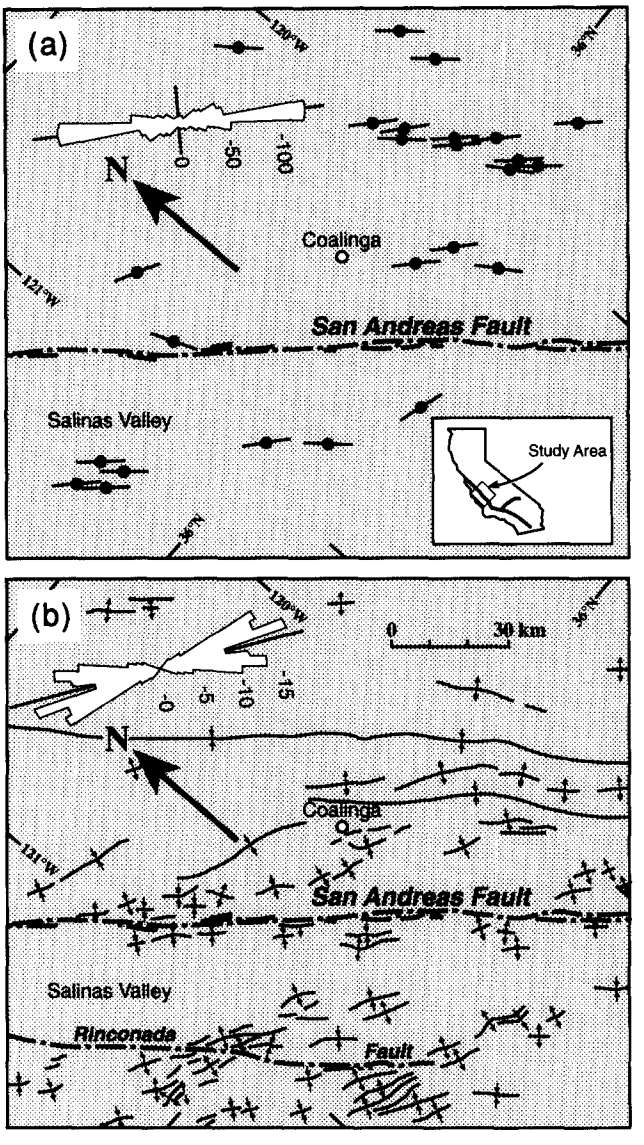

Fig. 11. Map summarizing the angular relationships between the mean azimuths of the San Andreas fault (139.8° ± 1.0°), after Mount & Suppe (1987). (a) Borehole breakouts (133.9° ± 1.9°), and (b) axes of young folds (127.9° ± 2.8°), in central California.

and Rinconada faults may be active at slow slip rates (Graham and Dickinson 1978, Sedlock and Hamilton 1991) and dextral strike-slip faults on the eastern side of the Sierra Nevada have apparently been active at a level of 5–8 mm y^{-1} through Quaternary time (Dokka and Travis 1990, Pezzopane and Weldon 1993). If the dextral motion on these faults is included, up to 88% of the discrete slip on the larger San Andreas fault system approaches that predicted by the strain modeling. Slip on subsidiary faults (Rymer *et al.* 1984), which are numerous in California (in contrast to Sumatra), could add significantly to discrete slip.

However, a discrepancy will always exist between slip on discrete major faults and plate motion as long as some wrenching is accommodated by deformation in the borderlands adjacent to these major faults. The systematic obliquity of structures—such as young folds and borehole breakouts—on either side of the San Andreas fault implies that a certain percentage of the wrench movement imposed by plate motion is accommodated in a

broad zone from the Coast Ranges to the Great Valley (Mount & Suppe 1992). Using a homogeneous transpressional model in the wrench 'borderland' adjacent to the fault in central California, Jamison (1991) estimated that 8.5 km of wrench motion are recorded in the folds adjacent to the San Andreas fault. Although this distributed shear component represents only 3% of the lateral motion imposed by plate motion, this value correlates well with the modeling of instantaneous strain which predicts that over 95% should be accommodated by discrete slip. Another test of the strain modeling involves the contractional structures in the 'borderlands' of the major faults. Recent structural studies suggest that the accumulated shortening normal to the fault is directly comparable to the normal component of shortening induced by the oblique plate convergence (Namson & Davis 1988, Bloch *et al.* 1993). Given the internal consistency between plate-motion vector orientation, obliquity of structures, and rate of slip on faults, a bulk transpression model for the San Andreas fault system is justified, as suggested previously (e.g. Harbert 1991).

Using the model of partitioning in transpression, deformation patterns in central California can be predicted. Since so much of the transform movement imposed by relative plate motions is taken up along discrete faults, the remaining crustal blocks adjacent to the San Andreas fault should be characterized by pure-shear dominated transpression. Mount & Suppe (1987) concluded, on the basis of geological and geophysical features, that $\dot{s}_3$ (σ_1) and $\dot{s}_2$ (σ_2) lie in the horizontal plane, and $\dot{s}_1$ (σ_3) is vertical, consistent with our strain modeling.

We propose that bulk wrench-dominated transpression systematically results in complex deformation and effective partitioning primarily because the instantaneous and finite strain axes can be so differently oriented. In California, faults are activated according to the instantaneous wrenching, but the crust must also accommodate the finite normal shortening associated with the pure-shear component. Hence thrust faults must form, verging in a direction almost perpendicular to the San Andreas fault, at a high angle to the minimum axis of instantaneous strain. Once thrusts and folds are formed, and sedimentary basins are structured, it is not clear that the borehole breakouts in the sediments actually respond to regional instantaneous strain. The geometry and kinematics of active deformation in the sediments imposed by finite strain, such as stiff layers acting as stress guides, will necessarily influence the attitude of breakouts.

DISCUSSION

Partitioning of stress vs strain

Zoback *et al.* (1987) argued that the weakness of the San Andreas fault controls stress orientation and deformation in central California. Using a model of frictionless cracks, Zoback *et al.* (1987) demonstrated that the maximum compressive stress, i.e. instantaneous strain, must be either exactly perpendicular or parallel to the main fault zone. The model of the San Andreas fault as a weak fault in a strong crust also carries the assumption that the stress field is partitioned between the fault and the adjacent blocks. The fault is activated by different stress conditions than its surroundings, possibly due to the role of fluid pressure in the fault (Byerlee 1990, 1992, Rice 1992). This model is supported by the lack of a heat flow anomaly that should be generated by the San Andreas fault (Lachenbruch and Sass 1973, 1980).

In contrast, McKenzie and Jackson (1983) suggested that plate motion controls both deformation and stresses in areas of oblique plate convergence. Since principal stresses are likely to be nearly parallel or perpendicular to the Earth's surface, McKenzie and Jackson (1983) argued that deformation in the upper crust is partitioned between sets of dip-slip and strike-slip faults. Molnar (1992) applied the same analysis to the San Andreas fault system and pointed out that fluid pressure is apparently as high in the thrust faults of the Coast Ranges (Berry 1973) and Sacramento Valley (Unruh *et al.* 1992) as it is on the San Andreas fault. Molnar (1992) also argues that the lack of a heat flow anomaly is of second-order compared to the commonly overlooked, 200 km wide zone of high heat flow in central California. The possible overestimation of frictional properties of rocks in faults (Logan *et al.* 1992) would also tend to overemphasize the lack of a heat flow anomaly on the San Andreas fault. In addition, seismicity on the San Andreas fault is comparable to other plate-boundary faults, which is inconsistent with the concept of a 'frictionless' fault.

Therefore, the main argument in support of stress partitioning is based on the angular relations between the San Andreas fault and the principal stresses (or instantaneous strain axes) derived from adjacent structures. Our purely kinematic model, based entirely upon the consequences of boundary conditions (direction and amount of plate motion) and partitioning of slip, accurately predicts the orientation of active structures in central California. The internal consistency between the plate-motion vector and the obliquity of structures in both central California and Sumatra suggests that strain partitioning is a more general paradigm for understanding transpressional systems than the concept of a weak fault.

No rheological assumptions were made in our model about the San Andreas or the Great Sumatran faults. Therefore, this model does not distinguish whether these faults are, in any sense, 'weak'. Strain partitioning simply assumes that plate motion is the fundamental factor controlling deformation. The question then remains as to what controls the amount of partitioning of the wrench component of deformation on the San Andreas and Great Sumatran fault systems.

Coupling vs decoupling

Both Sumatra and central California have been interpreted as examples of mechanical decoupling, with

stresses perpendicular or parallel to an extremely weak fault (e.g. Mount & Suppe 1987, 1992). Decoupling implies independence of the contractional and transcurrent components of deformation and no mechanical 'communication' between crustal segments adjacent to major faults. The concept of decoupling is based on the 'weakness' of major strike-slip faults across which mechanical continuity is lost.

In contrast, Molnar (1992) proposed that shearing of the strong upper mantle mechanically couples both sides of the San Andreas fault. He proposed that the 200 km wide zone of high heat flow in central California is generated by distributed shearing of the strong lithospheric mantle. Evidence for coupling is also demonstrated in the physical experiments of Richard & Cobbold (1989, 1990). These sand experiments show that, during oblique convergence, strike-slip and reverse faults are active simultaneously. Since both types of faults form in the same material, deformation is clearly not partitioned because of fault weakness. In this case, the coupling of the deformation is interpreted to be caused by a viscous layer below the experiment (Molnar 1992). Notice that coupling does not imply that faults are rheologically 'strong', but merely that there is no special strength requirement of strike-slip faults in transpressional settings.

It is not possible on the basis of strain modeling alone, to determine whether deformation in Sumatra and central California reflects coupling or decoupling. However, modeling does provide a tool to compare these obliquely convergent boundaries. The Great Sumatran fault is relatively inefficient at partitioning strike-slip movement while the San Andreas fault is extremely efficient. Can this fundamental difference be explained in terms of intrinsic fault properties? The Great Sumatra fault is located adjacent to and within a magmatic arc which presumably acts as a major crustal weakness (Jarrard 1986); in this geodynamic context, the fault should be relatively efficient at partitioning the wrench movement. The relatively sluggish motion along the southern portion of the Great Sumatran fault suggests that fault property is not a dominant parameter controlling fault behavior. In addition, seismic activity on the efficient San Andreas fault is comparable to the Great Sumatran fault and other crustal-scale faults, and again, it is not clear that the intrinsic properties of the 'efficient' San Andreas fault are any different from other continental discontinuities.

What clearly differs in these cases is the angle of relative plate motion. The relative plate motion in Sumatra suggests a bulk pure-shear dominated transpression, while central California correlates with wrench dominated transpression. In pure-shear dominated transpression, strike-slip faults are required to accommodate the minor wrench motion but contractional faults are favored by the overall plate motion. In wrench-dominated transpression, strike-slip faults are favored by overall plate motions, although thrust faults must develop to accommodate the minor contraction. In both cases, reverse and strike-slip faults are simultaneously formed as part of the same transpressional system, and respond to the same boundary conditions. However, we would expect the efficiency of strike-slip faults to vary significantly. Strike-slip faults in wrench-dominated transpressional settings, such as the San Andreas fault system, are effective at accommodating the wrench component of plate motion because they are oriented favorably for slip relative to the plate motion vector. The Great Sumatran fault and other strike-slip faults in pure-shear dominated transpressional settings only accommodate a small portion of the wrench component of plate motion since they form in response to a simple shear component of the finite strain deformation. Therefore, we predict a substantial change in fault efficiency around 20° relative plate motion which represents the transition between pure-shear and wrench-dominated transpression (Fig. 6).

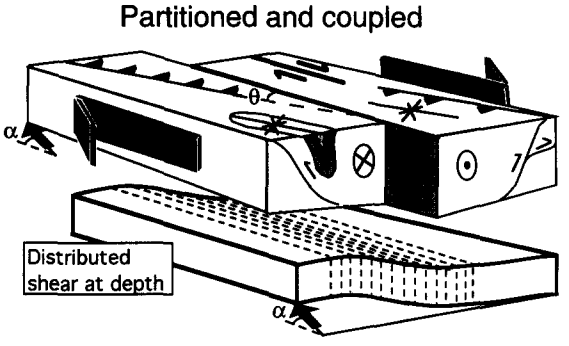

Fig. 12. Cartoon of kinematic strain partitioning. Partitioning of discrete slip in the upper crust is controlled by plate motion in a system where the adjacent sides of the main fault are mechanically coupled as a result of distributed shear at depth.

This hypothesis would require that the adjacent sides of major fault zones be coupled, in a mechanical sense. The strike-slip and reverse faults are all part of one transpressional system that responds to imposed plate motion. The consistency of orientation of geologic structures from 100–300 km, on both sides of these large faults in central California and Sumatra, supports this contention. Furthermore, the obliquity of these structures suggests that a component of strike-slip deformation is preserved in the wrench borderlands of each of these faults (Jamison 1991) which is not consistent with the idea of a 'weak' fault. While large strike-slip faults cause some reorientation of the stress field, this phenomenon is limited to the immediate vicinity of the faults (e.g. Bürgmann 1991). We maintain that these effects are only of second-order, and that, in general, slip on discrete faults and diffuse deformation in adjacent segments are coupled in transpressional zones. Lithospheric-scale deformation is controlled by boundary conditions imposed by plate motion, and not by fault properties.

One possible source of coupling, proposed by Molnar (1992) for the San Andreas system, is a layer of strong upper mantle that undergoes distributed shear (Fig. 12). In addition, the substantial seismic anisotropy within the upper mantle, presumably produced by ductile shearing, has been suggested in a variety of obliquely conver-

gent settings (e.g. Vauchez & Nicolas 1991). However, coupling might also be a crustal phenomenon, due to restrictions of strain compatibility and vertical rheological variations. The fundamental aspect of plate tectonics, that of rigid, decoupled plates separated by discrete boundaries, does not apply to continental settings (Molnar 1988). Therefore, distributed deformation in the mantle may not be the sole source of coupling. We propose that partitioning of the displacement field within the crust itself is another expression of mechanical coupling.

CONCLUSIONS

(1) Strain modeling of homogeneous transpression, using a three-dimensional velocity gradient tensor, allows wrench-dominated and pure-shear dominated transpression to be defined. This distinction is important because the relationship between instantaneous strain and finite strain, and the resultant geological structures, are very different for the two cases.

(2) Modeling shows that, in transpressional settings, the angle of convergence is not parallel to the direction of the compressive instantaneous strain (correlative with maximum compressive stress).

(3) In pure-shear dominated transpression, instantaneous strains are oriented consistently with reverse faults, although strike-slip faults must form to accommodate the finite strain associated with plate motion. Likewise, in wrench-dominated transpression, instantaneous strains are oriented consistently with movement on strike-slip faults. However, thrust faults must develop in these settings in response to the finite strain. Therefore, thrusts and strike-slip faults are active simultaneously in transpressional systems, although they respond to constant boundary conditions. Thus, large-scale faults are better described by the three-dimensional velocity gradient tensor and are controlled by the relative movement of material points, rather than the applied instantaneous strains.

(4) Models of partitioning of the displacement field provide templates that relate angle of plate convergence, orientation of the instantaneous strain axes, and relative degree of partitioning (amount of strike slip accommodated by discrete faults). The templates offer a predictive tool to evaluate the degree of partitioning within zones of oblique convergence and are internally consistent when applied to transpressive settings.

(5) Application of the partitioning analysis to a pure-shear dominated plate boundary (Sumatra) shows that the orientation of instantaneous structures is consistent with a low degree of displacement partitioning onto the Great Sumatran fault. The San Andreas fault displays a larger degree of displacement partitioning of the imposed plate motion.

(6) The modeling is purely kinematic and makes no assumptions about physical properties of the faults. Modeling demonstrates that plate motion can account for the pattern of instantaneous strain, regardless of whether the crustal blocks are coupled or decoupled on adjacent sides of the fault.

(7) We propose as a hypothesis that the factor controlling the efficiency of partitioning is the angle of relative plate motion. Pure-shear dominated transpressional settings ($20° < \alpha < 90°$), such as Sumatra, are inefficient at accommodating strike-slip movement. Here, the plate motion results in instantaneous strain values consistent with contractional deformation. In wrench-dominated transpression ($0° < \alpha < 20°$), such as central California, partitioning into discrete strike-slip movement is very efficient. The strike-slip faults are oriented favorably to accommodate the movement imposed by relative plate motion. In our view, it is not necessary to invoke any fault rheology to explain the orientation of structures in central California and Sumatra.

Acknowledgements—We would like to thank H. Fossen, P. Hudleston, P. Umhoefer and S. Wojtal for insightful discussions, and W. Unzog and two anonymous reviewers for critical reviews of the manuscript. This work was partially supported by NSF EAR-9305262 grant to C.T. and a Doctoral Dissertation Fellowship (Graduate School, University of Minnesota) to B.T.

REFERENCES

Anderson, E. M. 1951. *The Dynamic of Faulting*. Edinburgh. Oliver and Boyd,

Bellier, O., Sebrier, M. & Pramumijoyo, S. 1991. La grande faille de Sumatra: Géometrie, cinématique et quantité de déplacement mises en evidence par l'imagerie satellitaire. *C.r. Acad, Sci., Paris, Serie II*, **312**, 1219–1226.

Berry, F. A. F. 1973. High fluid potentials in the California Coast Ranges and their tectonic significance. *Bull. Am. Ass. Petrol. Geol.* **57**, 1219–1249.

Bloch, R. B., Huene, R. V., Hart, P. E. & Wentworth, C. M. 1993. Style and magnitude of tectonic shortening normal to the San Andreas fault across the Pyramid Hills and Kettleman Hill South Dome, California. *Bull. geol. Soc. Am.* **105**, 464–478.

Bobyarchick, A. R. 1986. The eigenvalues of steady flow in Mohr space. *Tectonophysics* **122**, 35–51.

Bürgmann, R. 1991. Transpression along the Southern San Andreas fault, Durmid Hill, California. *Tectonics* **10**, 1152–1163.

Byerlee, J. 1990. Friction, overpressure and fault normal compression. *Geophys. Res. Lett.* **17**, 2109–2112.

Byerlee, J. 1992. The change in orientation of subsidiary shears near faults containing pore fluid under high pressure. *Tectonophysics* **211**, 295–303.

Cashman, S. M., Kelsey, H. M., Erdman, C. F., Cutten, H. N. C. & Berryman, K. R. 1992. Strain partitioning between structural domains in the forearc of the Hikurangi subduction zone, New Zealand. *Tectonics* **11**, 242–257.

Curray, J. R., Moore, D. G. Lawver, L. A., Emmel, F. J., Raitt, R. W., Henry, M. & Kieckhefer, R. M. 1979. Tectonics of the Andaman sea and Burma. In: *Geological and Geophysical Investigations of Continental Margins* (edited by Watkins, J. S. *et al.*). *Am. Ass. Petrol. Geol.* **29**, 189–198.

DeMets, C., Gordon, R.G., Argus, D.F. & Stein, S. 1990. Current plate motions. *Geophys. J.* **101**, 425–478.

Diament, M., Harjono, H., Karta, K., Deplus, C., Dahrin, D., Zen, M. T., Gerard, M., Lassal, O., Martin, A. & Malod, J. 1992. Mentawai fault zone off Sumatra: a new key to the geodynamics of western Indonesia. *Geology* **20**, 259–262.

Dokka, R. K. & Travis, C. J. 1990. Late Cenozoic strike-slip faults of the central Mojave Desert, California. *Tectonics* **9**, 311–340.

Eberhart Phillips, D., Lisowski, M. & Zoback, M. D. 1990. Crustal

strain near the Big Bend of the San Andreas fault: analysis of the Los Padres-Tehachapi Trilateration Networks, California. *J. geophys. Res.* **95**, 1139–1153.
Flinn, D. 1979. The deformation matrix and the deformation ellipsoid. *J. Struct. Geol.* **1**, 299–307.
Fitch, J. T. 1972. Plate convergence, transcurrent faults, and internal deformation adjacent to Southeast Asia and the Western Pacific. *J. geophys. Res.* **77**(23), 4432–4460.
Fossen, H. & Tikoff, B. 1993. The deformation matrix for simultaneous pure shear, simple shear, and volume change, and its application to transpression/transtension tectonics. *J. Struct. Geol.* **15**, 413–422.
Graham, S. A. & Dickinson, W. R. 1978. Evidence for 115 kilometers of right slip on the San Gregorio-Hosgri fault trend. *Science, N.Y.* **199**, 179–181.
Harbert, W. 1991. Late Neogene relative motions of the Pacific and North American plates. *Tectonics* **10**, 1–16.
Jackson, J. 1992. Partitioning of strike-slip and convergent motion between Eurasia and Arabia in Eastern Turkey and the Caucasus. *J. geophys. Res.* **97**, 12471–12479.
Jamison, W. R. 1991. Kinematics of compressional fold development in convergent wrench terranes. *Tectonophysics* **190**, 209–232.
Jarrard, R. D. 1986. Terrane motion by strike-slip faulting of forearc slivers. *Geology* **14**, 780–783.
Karig, D. E., Lawrence, M. B., Moore, G. F. & Curray, J. R. 1980. Structural framework of the fore-arc basin, NW Sumatra. *Geol. Soc. Lond.* **137**, 77–91.
Lachenbruch, A. H. & Sass, J. H. 1973. Thermo-mechanical aspects of the San Andreas fault system. In: *Proc. Cong. on Tectonic Problems of the San Andreas Fault System*, Geological Sciences XIII, 192–205, Stanford University.
Lachenbruch, A. H. & Sass, J. H. 1980. Heat flow and energetics of the San Andreas fault zone. *J. geophys. Res.* **85**, 6185–6222.
Lassal, O., Huchon, P. & Harjono, H. 1989. Extension crustale dans le detroit de la Sonde (Indonesie). Donnees de la sismique reflexion (campagne Krakatoa). *C.r. Acad. Sci., Paris, Serie II* **309**, 205–212.
Logan, J. M., Dengo, C. A., Higgs, N. G. & Wang, Z. Z. 1992. Fabrics of experimental fault zones: their development and relationship to mechanical behavior: In: *Fault Mechanics and Transport Properties of Rocks* (edited by Evans, B. & Worp, T. F.). Academic Press, 33–67.
Malvern, L. E. 1969. *Introduction to the Mechanics of a Continuous Medium*. Prentice-Hall, Englewood Cliffs, New Jersey.
McCaffrey, R. 1991. Slip vectors and stretching of the Sumatran fore arc. *Geology* **19**, 881–884.
McKenzie, D. & Jackson, J. 1983. The relationship between strain rates, crustal thickening, paleomagnetism, finite strain and fault movements within a deforming zone. *Earth Planet. Sci. Lett.* **65**, 182–202.
Minster, J. B. & Jordan, T. H. 1978. Present-day plate motions. *J. geophys. Res.* **83**, 5331–5354.
Molnar, P. 1988. Continental tectonics in the aftermath of plate tectonics. *Nature* **335**, 131–137.
Molnar, P. 1992. Brace-Goetze strength-profiles, the partitioning of strike-slip and thrust faulting at zones of oblique convergence, and the stress-heat flow paradox of the San Andreas fault. In: *Fault Mechanics and Transport Properties of Rocks* (edited by Evans, B. & Wong, T.F.). 435–459, Academic Press, New York.
Moore, G. F., Curray, J. R. & Moore, D. G. 1980. Variations in geologic structure along the Sunda fore arc, northeastern Indian Ocean. *Am. Geophys. Union, Monograph.* **23**, 145–160.
Mount, V. S. & Suppe, J. 1987. State of stress near the San Andreas fault: implications for wrench tectonics. *Geology* **15**, 1143–1146.
Mount, V. S. & Suppe, J. 1992. Present-day stress orientations adjacent to active strike-slip faults: California and Sumatra. *J. geophys. Res.* **97**, 11,995–12,013.
Namson, J. S. & Davis, T. L. 1988. Seismically active fold and thrust belt in the San Joaquin Valley, central California. *Bull. geol. Soc. Am.* **100**, 257–273.
Oldow, J. S. 1990. Transpression, orogenic float, and lithospheric balance. *Geology* **18**, 991–994.
Oldow, J. S., Bally, A. W., Ave Lallemant, H. G. & Leeman, W. P. 1989. Phanerozoic evolution of the North American Cordillera: United States and Canada. In: *The Geology of North America: An Overview* (edited by Bally, A. W. & Palmer, A. R.). *Bull. geol. Soc. Am.* Boulder, 139–232.
Passchier, C. W. 1988. Analysis of deformation paths in shear zones. *Geol. Rdsch.* **77**(1), 309–318.
Pezzopane, S. K. & Weldon, R. J. 1993. Tectonic role of active faulting in central Oregon. *Tectonics* **12**, 1140–1169.
Pinet, N. & Cobbold, P. R. 1992. Experimental insights into the partitioning of motion within zones of oblique subduction. *Tectonophysics* **206**, 371–388.
Powell, R. E. & Weldon, R. J. 1992. Evolution of the San Andreas fault. *Annu. Rev. Earth & Planet. Sci.* **20**, 431–468.
Prescott, W. H. & Yu, S.-B. 1986. Geodetic measurement of horizontal deformation in the northern San Francisco Bay region, California. *J. geophys. Res.* **86**, 7475–7484.
Ramberg, H. 1975. Particle paths, displacement and progressive strain applicable to rocks. *Tectonophysics* **28**, 1–37.
Ramsay, J. G. & Graham, R. H. 1970. Strain variation in shear belts. *Can. J. Earth Sci.* **7**, 786–813.
Rice, J. R. 1992. Fault stress states, pore pressure distributions, and the weakness of the San Andreas fault. In: *Fault Mechanics and Transport Properties of Rocks* (edited by Evans, B. & Wong, T. F.). 435–459, Academic Press, New York.
Richard, P. & Cobbold, P. 1989. Structures en fleur positives et décrochements crustaux: modélisation analogique et interprétation mécanique. *C.r. Acad. Sci., Paris, Série II* **308**, 553–560.
Richard, P. & Cobbold, P. 1990. Experimental insights into partitioning of fault motions in continental convergent wrench zones. *Ann. Tect.* **IV**, 35–44.
Rymer, M. J., Lisowski, M. & Burford, R. O. 1984. Structural explanation for low creep rates on the San Andreas fault near Monarch Peak, Central California. *Bull. seis. Soc. Am.* **74**, 925–931.
Sanderson, D. & Marchini, R. D. 1984. Transpression. *J. Struct. Geol.* **6**, 449–458.
Sedlock, R. L. & Hamilton, D. H. 1991. Late Cenozoic tectonic evolution of southwestern California. *J. geophys. Res.* **96**, 2325–2351.
Simpson, C. & De Paor, D. G. 1993. Strain and kinematic analysis of general shear zones. *J. Struct. Geol.* **15**, 1–20.
Tikoff, B. & Fossen, H. 1993. Simultaneous pure and simple shear: the unifying deformation matrix. *Tectonophysics* **217**, 267–283.
Tikoff, B. & Teyssier, C. 1993. Highly transpressive tectonics and emplacement of granitoids between en échelon *P*-fractures: east central Sierra Nevada batholith, California: Geol. Soc. Am. prog. with abstracts, Cord. and Rocky Mtn. section.
Tron, V. & Brun, J.-P. 1991. Experiments on oblique rifting in brittle–ductile systems. *Tectonophysics* **188**, 71–84.
Truesdell, C. 1953. Two measures of vorticity. *J. Rational Mech. Anal.* **2**, 173–217.
Unruh, J. R., Davisson, M. L., Criss, R. E. & Moore, E. M. 1992. Implications of perennial saline springs for abnormally high fluid pressures and active thrusting in western California. *Geology* **20**, 431–434.
Vauchez, A. & Nicolas, A. 1991. Mountain building: strike-parallel displacements and mantle anisotropy. *Tectonophysics* **185**, 183–201.
Walcott, R. I. 1984. Geodetic strain and large earthquakes in the axial tectonic belt of North Island, New Zealand. *J. geophys. Res.* **83**, 4419–4429.
Weijermars, R. 1991. The role of stress in ductile deformation. *J. Struct. Geol.* **13**, 1061–1078.
Weldon, R. & Humphreys, E. 1986. A kinematic model of southern California. *Tectonics* **5**, 33–48.
Withjack, M. O. & Jamison, W. R. 1986. Deformation produced by oblique rifting. *Tectonophysics* **126**, 99–124.
Wojtal, S. 1989. Measuring displacement gradients and strains in faulted rocks. *J. Struct. Geol.* **11**, 669–678.
Zoback, M. D. & Healy, J. H. 1992. *In situ* stress measurements to 3.5 km depth in the Cajon Pass scientific research borehole: implications for the mechanics of crustal faulting. *J. geophys. Res.* **97**, 5039–5057.
Zoback, M. D., Zoback, M. L., Mount, V. S., Suppe, J., Eaton, J. P., Healy, J. H., Oppenheimer, D., Reasenberg, P., Jones, L., Raleigh, C. B., Wong, I. G., Scotti, O. & Wentworth, C. 1987. New evidence on the state of stress of the San Andreas fault system. *Science, N.Y.* **238**, 1105–1111.

APPENDIX 1

α = angle between contractional flow apophysis and x-direction; correlated with angle of relative plate movement.
$\mathbf{D}$ = deformation matrix (or deformation tensor).
$\dot{\varepsilon}_i$ = pure shear strain rate.
$\dot{\gamma}$ = simple shear strain rate.
γ = shear strain (simple shear component of finite strain).

Γ = effective shear strain.
ISA = instantaneous stretching axes, equal to instantaneous strain axes.
k_n = pure shear components.
λ_n = axes of finite strain ellipsoid, eigenvalues of the matrix $\mathbf{DD}^T$.
$\mathbf{L}$ = velocity gradient tensor.
R_e = ratio of the long and short axes of the finite strain ellipsoid.
$\dot{s}_i$ = principal strain-rates, eigenvalues of the matrix $\dot{\mathbf{S}}$.
$\dot{\mathbf{S}}$ = stretching (or rate of deformation) tensor.
θ = angle between the maximum horizontal axis of the instantaneous strain axes (either $\dot{S}_1$ or $\dot{S}_2$) and the x-co-ordinate axis.
W_k = kinematic vorticity number.
z = vertical co-ordinate axis.

APPENDIX 2

Homogeneous transpressional deformation is described by the deformation matrix.

$$\mathbf{D} = \begin{pmatrix} 1 & \dfrac{\gamma(1-k)}{\ln(k^{-1})} & 0 \\ 0 & k & 0 \\ 0 & 0 & k^{-1} \end{pmatrix} \tag{A1}$$

where k is the amount of pure shear component that acts in the horizontal (x) direction which is compensated by elongation k^{-1} in the vertical (z) direction. The term γ is the simple shear component of deformation.

To avoid compatibility problems, the pure shear component of deformation must be the same within and adjacent to a deforming zone (e.g. Ramsay & Graham 1970). In our matrix, the offset due to the simple shear component is given by the effective shear strain, Γ (Tikoff & Fossen 1993). For a homogeneous deformation, Γ is given by the equation:

$$\Gamma = \frac{\gamma(1-k)}{\ln(k^{-1})} \tag{A2}$$

and since k is constant throughout deformation, Γ can be written as:

$$\Gamma = \gamma(\text{Constant}). \tag{A3}$$

To partition the deformation, we simply partition the total effective shear strain into components of homogeneous deformation and discrete slip:

$$\begin{aligned} \Gamma_{\text{total}} &= \gamma_{\text{total}}\,(\text{Constant}) \\ &= (\gamma_{\text{homogeneous deformation}} + \gamma_{\text{discrete slip}})\,(\text{Constant}) \\ &= \Gamma_{\text{homogeneous deformation}} + \Gamma_{\text{discrete slip}}. \end{aligned} \tag{A4}$$

As deformation is partitioned into discrete slip, deformation in the zone of homogeneous strain becomes closer to pure shear. Therefore, if enough partitioning onto discrete slip occurs in a wrench-dominated transpressional setting, the style of deformation adjacent to discrete faults will appear to be pure-shear dominated transpression. This apparently occurs in central California, adjacent to the San Andreas fault.